FULL PAPERS

Magnetic Resonance in Medicine 64:334–340 (2010)

^{1}H-[^{13}C] NMR Spectroscopy of the Rat Brain During Infusion of [2-^{13}C] Acetate at 14.1 T

Lijing Xin,[1] Vladimír Mlynárik,[1] Bernard Lanz,[2] Hanne Frenkel,[2] and Rolf Gruetter[1–3]*

Full signal intensity ^{1}H-[^{13}C] NMR spectroscopy, combining a preceding ^{13}C-editing block based on an *inversion* BISEP (B_1-insensitive spectral editing pulse) with a spin-echo coherence–based localization, was developed and implemented at 14.1 T. ^{13}C editing of the proposed scheme was achieved by turning on and off the ^{13}C adiabatic full passage in the ^{13}C-editing block to prepare inverted and noninverted ^{13}C-coupled ^{1}H coherences along the longitudinal axis prior to localization. The novel ^{1}H-[^{13}C] NMR approach was applied in vivo under infusion of the glia-specific substrate [2-^{13}C] acetate. Besides a ~50% improvement in sensitivity, spectral dispersion was enhanced at 14.1 T, especially for J-coupled metabolites such as glutamate and glutamine. A more distinct spectral structure at 1.9–2.2 ppm(parts per million) was observed, e.g., glutamate C3 showed a doublet pattern in both simulated ^{1}H spectrum and in vivo ^{13}C-edited ^{1}H NMR spectra. Besides ^{13}C time courses of glutamate C4 and glutamine C4, the time courses of glutamate C3 and glutamine C3 obtained by ^{1}H-[^{13}C] NMR spectroscopy were reported for the first time. Such capability should greatly improve the ability to study neuron-glial metabolism using ^{1}H-observed ^{13}C-edited NMR spectroscopy. Magn Reson Med 64:334–340, 2010. © **2010 Wiley-Liss, Inc.**

Key words: ^{1}H-[^{13}C] NMR spectroscopy; [2-^{13}C] acetate; glutamate; glutamine; rat brain

Dynamic detection of ^{13}C label incorporation by ^{13}C NMR spectroscopy in conjunction with ^{13}C label administration allows the investigation of neuroglial metabolism in vivo (see de Graaf et al. (1) and Gruetter et al. (2). for reviews). By dynamically measuring ^{13}C incorporation into different carbon positions of NMR-detectable metabolic products such as glutamate (Glu) and glutamine (Gln) during the infusion of labeled substrate and then fitting this dynamic information with a suitable mathematical model, several crucial metabolic fluxes, e.g., exchange rate between 2-oxoglutarate and Glu, the tricarboxylic acid (TCA) cycle rate and the Glu-Gln cycle rate, can be quantitatively derived (3–5). Generally, ^{13}C-enriched glucose, such as [1-^{13}C] or [1, 6-$^{13}C_2$] glucose, has been used as the substrate (6,7).

In the last two decades, ^{13}C-labeled acetate (Ace) has been employed in a few ^{13}C NMR studies (8–17). Since Ace is taken up exclusively by astrocytes (18), the glial Gln pool will be labeled prior to the larger neuronal Glu pool (19). Hence, ^{13}C-labeled Ace infusion could potentially increase the accuracy of the assessment of the Glu-Gln cycle rate and the TCA cycle rate in astrocytes (20). However, due to the smaller pool size of Gln (~3 μmol/g) (21) and strong labeling dilution effect of the neuronal Glu, ^{13}C-labeled signals are much smaller when using Ace infusion compared to those acquired with glucose infusion, which increases demands on the measurement sensitivity. To date, the dynamic ^{13}C labeling time courses reported by in vivo studies using ^{13}C-labeled Ace were limited to the measurement of the C4 position of Glu and Gln (11,22).

The measurement of ^{13}C labeling has been achieved using either direct or indirect ^{13}C NMR detection (3,6,23–25). Direct detection of ^{13}C NMR signals allows the individual measurement of turnover of C2, C3, and C4 positions of Glu and Gln due to the large chemical-shift dispersion of the ^{13}C spectral lines. However, the inherently low sensitivity of ^{13}C limits the spatial resolution to ~400 μL (26). To increase the sensitivity, indirect detection of ^{13}C through the more sensitive ^{1}H nuclei is an alternative, albeit at the expense of a lower spectral resolution, such as the partial separation of labeling in Glu and Gln (23,25), which limits the achievable dynamic information and the reliability of the two-compartment metabolic modeling (20). For instance, Pfeuffer et al. (23) proposed a modified stimulated echo acquisition mode localization for performing adiabatic carbon editing and decoupling, and demonstrated the measurement of GluC4 and GlnC4 time courses with glucose infusion at 9.4 T. A proton-observed carbon-edited NMR sequence (7) based on three-dimensional image-selected in vivo spectroscopy localization was performed with glucose infusion at 7 T in rat brain, and the reported time courses were limited to GluC4, GlnC4, and GluC3 + GlnC3 (27).

By further increasing the magnetic field strength, the signal-to-noise ratio and spectral resolution of ^{1}H-[^{13}C] NMR spectroscopy are improved, especially for J-coupled metabolites (28), which will potentially lead to the measurement of additional labeling information, e.g., GluC3 and GlnC3 time courses.

In the present study, a full signal intensity ^{1}H-[^{13}C] NMR spectroscopy, combining the spin-echo coherence-based localization "SPECIAL" (SPin ECho, full Intensity

[1]Laboratory of Functional and Metabolic Imaging, Ecole Polytechnique Fédérale de Lausanne, Lausanne, Switzerland.

[2]Department of Radiology, University of Lausanne, Lausanne, Switzerland.

[3]Department of Radiology, University of Geneva, Geneva, Switzerland.

Grant sponsor: Swiss National Science Foundation; Grant number: SNF 3100A0-116220.

*Correspondence to: Rolf Gruetter, Ph.D., Ecole Polytechnique Fédérale de Lausanne, SB-LIFMET, CH F0 632, Station 6, CH-1015 Lausanne, Switzerland. E-mail: rolf.gruetter@epfl.ch

Received 20 July 2009; revised 11 November 2009; accepted 23 December 2009.

DOI 10.1002/mrm.22359

Published online in Wiley InterScience (www.interscience.wiley.com).

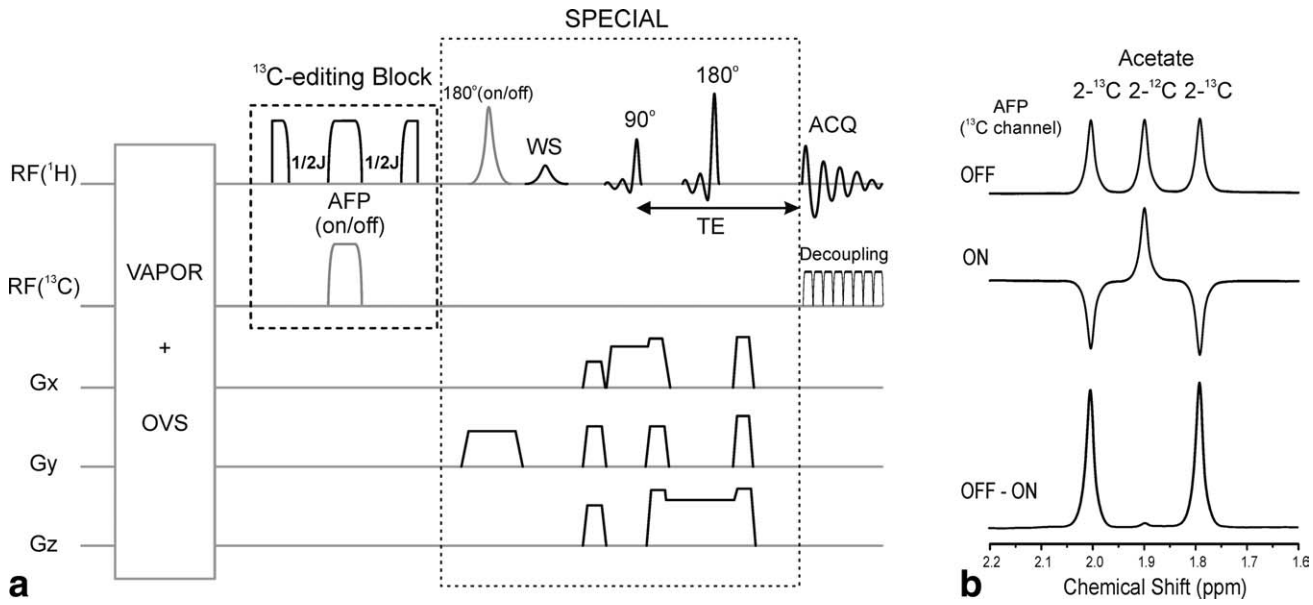

FIG. 1. **a:** The sequence diagram of SPECIAL-BISEP (TE = 2.8 ms). The editing was achieved by applying an AFP in the ^{13}C channel on alternate scans. **b:** In vitro validation of the editing scheme was performed at 14.1 T on a solution of 67% enriched [2-^{13}C] sodium Ace (no ^{13}C decoupling during the acquisition was applied). When the ^{13}C AFP is turned off, the *inversion* BISEP pulse acts as a 0° BIR-4 pulse (top), while when AFP is turned on, ^{13}C-coupled ^{1}H resonances are inverted (middle). In the difference spectrum (bottom), the uncoupled resonances (^{1}H-[2-^{12}C]) are minimized and only the ^{13}C-coupled ^{1}H resonances (^{1}H-[2-^{13}C]) are detected.

Acquired Localized spectroscopy) (29) with a preceding ^{13}C-editing block based on an *inversion* BISEP (B_1-insensitive spectral editing pulse) (30), was implemented at an ultrahigh magnetic field strength of 14.1 T and validated in vitro and in vivo during infusion of [2-^{13}C] Ace. We further demonstrated improved ^{1}H-[^{13}C] NMR spectral resolution at 14.1 T and feasibility of measuring individual time courses of GluC4, GlnC4, GluC3, and GlnC3.

MATERIALS AND METHODS

Animal Preparation

All animal preparation procedures were performed according to local and federal guidelines and were approved by the local ethics committee. Six healthy Sprague-Dawley rats (263 ± 19 g, mean ± standard deviation) were fasted overnight (15–16 h), with free access to water before the studies. Animals were intubated and ventilated by 2% isoflurane during the surgery. Both femoral veins were catheterized for continuous infusion of α-chloralose (Fisher Scientific, Pittsburgh, PA) and 99% enriched [2-^{13}C] sodium Ace (Sigma-Aldrich, St. Louis, MO). One femoral artery was cannulated for blood sampling. After preparation, anesthesia was achieved by an 80 mg/kg initial bolus of α-chloralose, followed by continuous infusion at a rate of ~26.7 mg/kg/h. The animal was placed in a homemade holder and the head was stereotaxically fixed. Respiration rate and blood pressure were continuously monitored (SA Instruments Inc., NY). Body temperature was measured by a rectal thermosensor and maintained at 38.0 ± 0.5°C by circulating heated water. A variable bolus of 3-M 99% enriched [2-^{13}C] sodium Ace (pH = 6) was given over two consecutive 5-min periods, with rates of 1.8 mmol/min/kg and 1.1 mmol/min/kg, respectively, and then a continuous rate of 0.3 mmol/min/kg was applied. The infused volume of Ace solution was ~5 mL in total. Arterial blood (200 μL) was sampled approximately every 30 min for monitoring blood gases (pCO_2 = 39 ± 2 mm Hg, pO_2 > 100 mm Hg), pH (7.41 ± 0.03), and the analysis of plasma Ace concentration and isotopic enrichment. An aliquot of arterial blood was immediately centrifuged and stored in a nearby −80°C freezer for subsequent processing. The total amount of blood draw was below 10% of the total blood volume of the rat.

Analysis of Blood Plasma and High-Resolution NMR Spectroscopy

Plasma samples were thawed and immediately centrifuged (12,000*g*) with a centrifugal filter with a molecular-weight cutoff of 10 kDa (Vivaspin 500; Sartorius AG, Goettingen, Germany). The ultrafiltrate of the plasma was lyophilized and dissolved in 400 μL D_2O containing 0.774 mM 3-(trimethylsilyl)propionic-2,2,3,3-d_4 acid sodium salt (sodium salt; Ciba Geigy AG, Basel, Switzerland), which was used as a chemical shift and internal concentration reference for high-resolution NMR spectroscopy. The measurements were performed on a 500-MHz vertical-bore spectrometer (Bruker, Fallanden, Switzerland). One-dimensional ^{1}H pulse-and-acquire was used to measure the isotopic enrichment and the concentration of Ace in the blood plasma (pulse repetition time = 15 sec).

^{1}H-[^{13}C] NMR Sequence

The proposed ^{1}H-[^{13}C] NMR sequence termed *SPECIAL-BISEP* was the combination of the SPECIAL localization sequence and a preceding ^{13}C-editing block based on the *inversion* BISEP (Fig. 1a).

The *inversion* BISEP, which was based on a segmented 0° BIR-4 (B_1-insensitive rotation with 4 segments) pulse with two pulse interval delays ($\tau = 1/2J$), consisted of three segments in the ^{1}H channel (time-reversed adiabatic half-passage [$\pi/2$, 0.5 ms], adiabatic full passage [AFP; π, 1 ms], and adiabatic half-passage [$\pi/2$, 0.5 ms]) and one AFP (1 ms) in the ^{13}C channel centered at the central segment of 0° BIR-4 pulse in the ^{1}H channel (30). The modulation functions of the AFP and adiabatic half-passage were based on hyperbolic tangent and tangent functions. Using product operator formalism to describe coherence evolution of ^{13}C (S)-coupled ^{1}H (I) spins at the end of the BISEP, the coherence is $I_z \cos(2\pi J\tau) - 2I_xS_z \sin(2\pi J\tau)$. When using the time delay $\tau = 1/2J$ ($J = 127$ Hz), $-I_z$ is obtained to achieve the inversion of ^{13}C-coupled ^{1}H coherences. On the other hand, without the AFP in the ^{13}C channel the ^{13}C-editing block acts as a 0° BIR-4 pulse and the coherence returns to $+I_z$. Therefore, by turning off (unedited) and on (edited) the AFP in the ^{13}C channel, $\pm I_z$ are prepared prior to the localization. Since the uncoupled signals (corresponding to protons bound to ^{12}C) undergo only segmented 0° BIR-4 pulse and return to the z axis in both unedited and edited acquisitions, the subtracted spectrum contained ^{1}H resonances bound to ^{13}C.

The bandwidth of the *inversion* BISEP was ~2 kHz (3.3 ppm at 14.1 T) in ^{1}H channel, where $\gamma B_{1max}/2\pi = 6.7$ kHz, and ~12 kHz (80 ppm at 14.1 T) at the ^{13}C frequency, where $\gamma B_{2max}/2\pi \geq 7$ kHz. The frequency offsets were set to the resonance frequencies of GluC4 protons and carbon (2.34 ppm and 35 ppm), respectively.

Following the ^{13}C-editing block, the SPECIAL localization sequence based on the combination of one-dimensional image-selected in vivo spectroscopy and slice-selective spin-echo (29) was used to detect the prepared $\pm I_z$ from a selected volume of interest. An ultrashort echo time (TE) of 2.8 ms was used to attain full signal intensity and minimize spectral evolution due to ^{1}H-^{1}H coupling. Outer volume suppression was achieved by six adiabatic hyperbolic secant pulses in three outer-volume-suppression modules interleaved with VAPOR (VAriable Pulse power and Optimized Relaxation delays) water suppression (31). An additional water-suppression pulse was implemented between one-dimensional image-selected in vivo spectroscopy and the spin-echo module. Adiabatic ^{13}C decoupling was based on an adiabatic hyperbolic secant (HS8) pulse applied with both MLEV-4 and a five-step phase cycling (23) during the 145-ms acquisition time.

In Vivo MRS and Quantification

All experiments were carried out on an animal MRI system (Varian, Palo Alto, CA) interfaced to a 14.1-T, 26-cm, horizontal-bore magnet (Magnex Scientific, Oxford, UK) with actively shielded gradients (12-cm inner diameter, 400 mT/m in 120 μs). A homemade 13 mm-diameter geometrically decoupled quadrature ^{1}H surface coil with a 10 mm-diameter single-loop linear ^{13}C coil was used as both transmitter and receiver. At the center of the ^{13}C coil, a sphere filled with 99% ^{13}C-enriched formic acid was placed to provide a reference signal for power calibration of the adiabatic pulses in the ^{13}C channel.

Fast spin-echo images (effective TE = 45 ms, echo train length = 8, pulse repetition time = 2.5 sec, number of transitions = 2, slice thickness = 1 mm, field of view = 30 × 30 mm^2, matrix = 256 × 256) were acquired for positioning of the volume of interest. Localized ^{1}H-[^{13}C] spectra were acquired from a volume of 144 μL (8 × 3 × 6 mm^3) centered in cerebral cortex of the rat brain. To optimize the magnetic field homogeneity in the volume of interest, an echo-planar imaging version of FASTMAP (32) was used to adjust all first- and second-order shims, which achieved a full width at half maximum of the water signal of 20–22 Hz in vivo.

During 150 min of 99% enriched [2-^{13}C] sodium Ace infusion, localized proton signal (64 averages, pulse repetition time = 4 sec) was continuously acquired with and without applying the ^{13}C AFP in an interleaved fashion. In vivo spectra were analyzed by LCModel (33). Two basis sets were employed: (i) a standard basis set for unedited ^{1}H spectra contained a measured macromolecular baseline and simulated metabolite spectra (34); (ii) a basis set for ^{13}C-edited ^{1}H NMR spectra contained simulated metabolite spectra of Ace C2, N-acetyl aspartate C6, Glu (C2, C3, and C4), Gln (C2, C3, and C4), γ-aminobutyric acid (C2, C3, and C4), aspartate (C2 and C3), and total creatine (C2 and C3). AceC2 (1.9 ppm) served as a reference for frequency and phase adjustment of the ^{13}C-edited ^{1}H spectra. After LCModel analysis, isotopic enrichment of metabolites such as GluC4, GlnC4, GluC3, GlnC3, and AceC2 was calculated directly from the relative concentration ratio of ^{13}C concentration obtained from ^{13}C-edited ^{1}H NMR spectra and the total concentration (^{12}C + ^{13}C) obtained from unedited ^{1}H spectra. Total creatine was assumed to be 8 μmol/g for calculating the absolute concentration (21,22).

Spectral Simulation of Glu and Gln

Proton spectra of Glu and Gln under spin-echo excitation at TE = 2.8 ms were simulated at three different magnetic field strengths of 7, 9.4, and 14.1 T. Quantum mechanics simulations, based on density matrix formalism, were performed in Matlab (version 7.5; The MathWorks, Inc., Natick, MA) (35). Published chemical shifts, i.e., 3.74 ppm (^{2}CH), 2.04 ppm and 2.12 ppm (^{3}CH$_2$), and 2.34 ppm and 2.35 ppm (^{4}CH$_2$) for Glu and 3.75 ppm (^{2}CH), 2.13 ppm and 2.11 ppm (^{3}CH$_2$), and 2.43 ppm and 2.45 ppm (^{4}CH$_2$) for Gln, and J-coupling constants (36) were used in the calculation. The line widths of metabolites were set to 8, 10, and 18 Hz for 7, 9.4, and 14.1 T, respectively.

RESULTS

Isotopic enrichment of AceC2 in the blood reached over 95% within 5 min after starting the infusion of 99% enriched [2-^{13}C] sodium Ace and was stable at around 90% during the whole experiment. The concentration of plasma Ace during the experiment was 9 ± 3 mM.

To validate the performance of the SPECIAL-BISEP scheme, a 20-mL plastic cylinder containing 200-mM [2-^{13}C] sodium Ace and 100-mM unlabeled sodium Ace was prepared. Applying the ^{13}C AFP at the ^{13}C

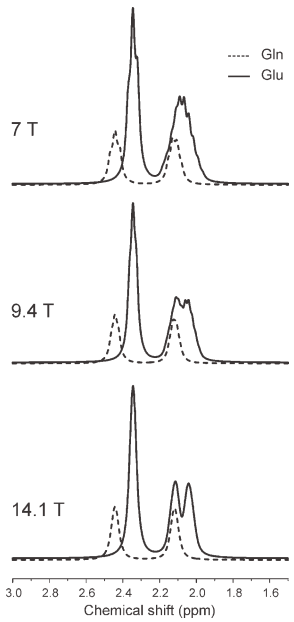

FIG. 2. Simulated ^{1}H spectra of Glu and Gln under spin-echo excitation at 7, 9.4, and 14.1 T, with line widths of 8, 10, and 18 Hz, respectively (TE = 2.8 ms). The concentration of Glu and Gln used in the simulation was 8.3 μmol/g and 2.7 μmol/g, respectively (21).

resonance of AceC2, the ^{13}C-coupled ^{1}H resonances were inverted (Fig. 1b, middle). When the ^{13}C AFP was turned off, ^{13}C-coupled ^{1}H resonances were detected in phase with the central ^{1}H-[^{12}C] resonances (Fig. 1b, top). Subtracting the noninverted spectrum (Fig. 1b, top) from the inverted spectrum (Fig. 1b, middle), uncoupled resonances were successfully eliminated and ^{13}C-coupled ^{1}H resonances were exclusively retained (Fig. 1b, bottom).

To demonstrate the improvement of spectral resolution for J-coupled metabolites at 14.1 T, ^{1}H spectra of Glu and Gln at different magnetic field strengths, i.e., 7, 9.4, and 14.1 T, were simulated (Fig. 2). Since the line width of the multiplets of Glu and Gln is mainly determined by the J-coupling constant, which is independent of the amplitude of static field, the spectral resolution was expected to be substantially improved, despite the increase in the singlet line width with the amplitude of static field. Note that at 14.1 T, the C3 of Glu was a more distinct doublet of its nonequivalent ^{1}H resonances at 2.04 ppm and 2.12 ppm compared to that at both 7 and 9.4 T.

To demonstrate the ^{1}H-[^{13}C] NMR editing scheme in vivo, NMR experiments in conjunction with [2-^{13}C] Ace infusion were performed. The in vivo unedited ^{1}H spectrum of rat brain acquired by SPECIAL-BISEP during infusion of [2-^{13}C] Ace demonstrated new spectral features at 14.1 T, such as better-separated spectral lines at 1.9–2.2 ppm, which correspond to Glu, Gln, N-acetyl aspartate, and Ace resonances (Fig. 3).

The 45-min averaged ^{13}C-edited ^{1}H NMR spectrum acquired 106 min after starting Ace infusion exhibited spectral features ascribed to multiplets of GluC3, GlnC3, and N-acetyl aspartate C6 (Fig. 3). In addition, the major resonance signal, i.e., GluC4 at 2.34 ppm, was clearly separated from the GlnC4 resonance at 2.44 ppm.

LCModel analysis performed using a basis set composed of the individual position of molecules resulted in

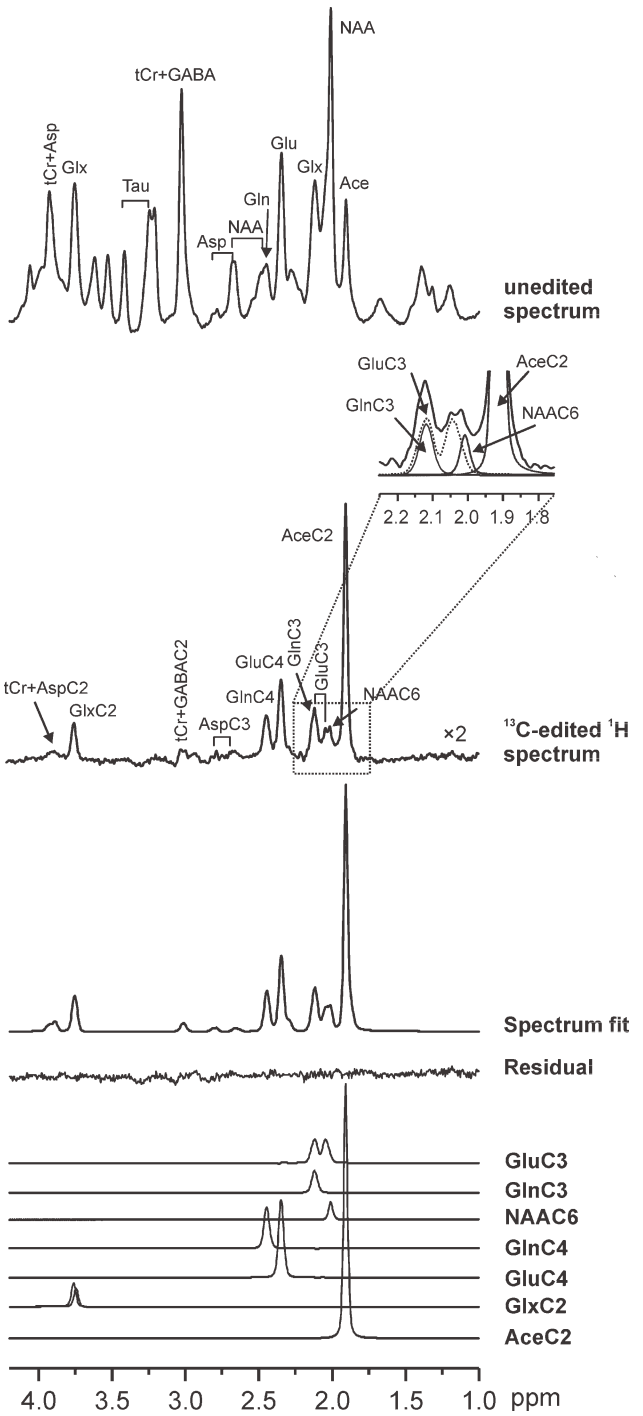

FIG. 3. Averaged unedited and edited ^{1}H-[^{13}C] NMR spectrum acquired in vivo at 14.1 T for 45 min after ~106 min of Ace infusion. Gaussian weighting function (exp [$-t^2/0.08^2$]) was applied before Fourier transformation. No baseline correction and water signal removal were applied. The fit of the ^{13}C-edited ^{1}H NMR spectrum, fit residual, and individual fit of Glu (C2, C3, and C4), Gln (C2, C3, and C4), AceC2 and N-acetyl aspartate (NAA) C6 are shown. A detailed region of in vivo ^{1}H-[^{13}C] NMR spectrum (thick line) and spectral fits (thin lines) is shown in the inset.

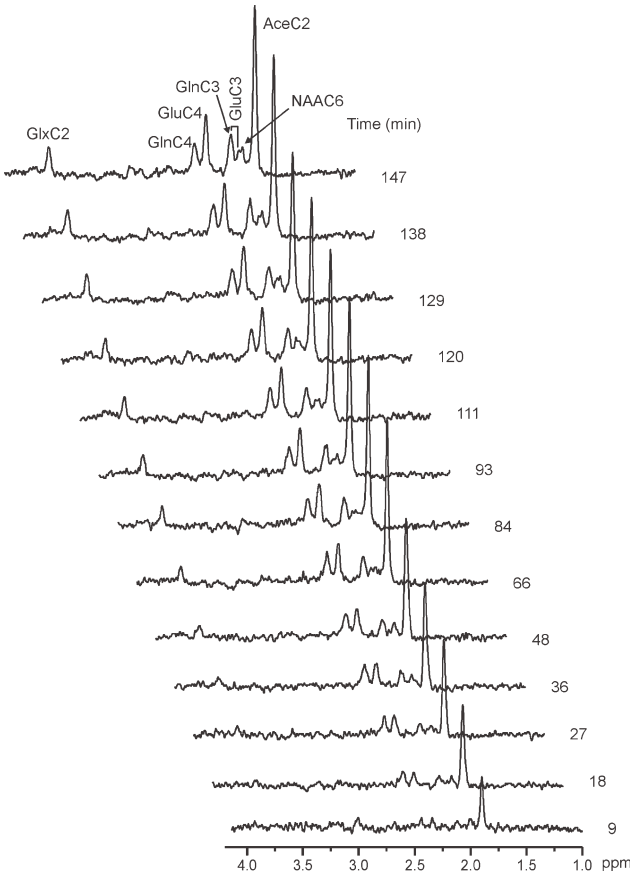

FIG. 4. Stack plot of time-resolved ^{13}C-edited ^{1}H spectra from the rat brain in vivo during [2-^{13}C] Ace infusion. Each spectrum was summed over ~9 min (number of transitions = 128) scans and gaussian weighting functions (exp [$-t^2/0.08^2$]) were applied. No baseline correction and water signal removal were applied. Data are from the same animal shown in Fig. 3.

an excellent fit of the ^{13}C-edited ^{1}H spectrum with minimal fit residual (Fig. 3). Note that GluC3 exhibited a distinct doublet structure expected from the two nonequivalent protons, as shown in the simulated spectrum (Fig. 2).

^{1}H-[^{13}C] NMR spectra summed every ~9 min (128 scans) demonstrated the dynamic ^{13}C incorporation (Fig. 4). From the stack plot, it is clear that after ^{13}C incorporation into AceC2, GlnC4 and GluC4 were labeled first, followed by labeling in the C3 and C2 position of Glu and Gln.

From the analysis of the unedited ^{1}H spectra and ^{13}C-edited ^{1}H spectra (64 averages), total concentration of metabolites (^{12}C + ^{13}C) and the concentration of ^{13}C-labeled metabolites were obtained. Cramer-Rao lower bounds (expressed in concentration unit) of the concentration of GluC4, GlnC4, GluC3, and GlnC3 were 0.047 ± 0.004 μmol/g, 0.048 ± 0.004 μmol/g, 0.13 ± 0.02 μmol/g, and 0.081 ± 0.009 μmol/g (mean ± standard deviation; n = 6), respectively, in 4.5-min spectra. Dynamic isotopic enrichment of GluC4, C3 and GlnC4, C3 was calculated by dividing the concentration of ^{13}C-labeled metabolites by the total concentration of the respective metabolites. All data points were used in the ^{13}C-label time courses. Average time courses of GluC4, C3 and GlnC4, C3 (n = 6) with a time resolution of ~4.5 min (each data point contains 64 scans) are shown in Fig. 5. At steady state, the isotopic enrichment of GluC4 and GlnC4 was 16% and 35%, respectively. The labeling of GluC3 and GlnC3 continued to increase during the whole experiment, and their isotopic enrichment reached 12% and 20% at ~150 min, respectively. A small increase in the isotopic enrichment of N-acetyl aspartate C6 was also observed (not shown) but remained below ~4% during the infusion experiment, which can be ascribed to its slow metabolism (37).

DISCUSSION

The present study introduced a novel ^{1}H-[^{13}C] NMR spectroscopic technique that attained full signal intensity by using a BISEP-based ^{13}C-editing block combined with the SPECIAL localization at ultrashort TE.

The 180° BISEP, originally introduced as a refocusing pulse (30), was used in the proposed scheme as a ^{13}C inversion pulse for inverting ^{13}C-coupled ^{1}H coherences on alternate scans prior to localization (Fig. 1a). As a ^{13}C-editing adiabatic pulse, BISEP enabled us to minimize the signal loss due to the inhomogeneous

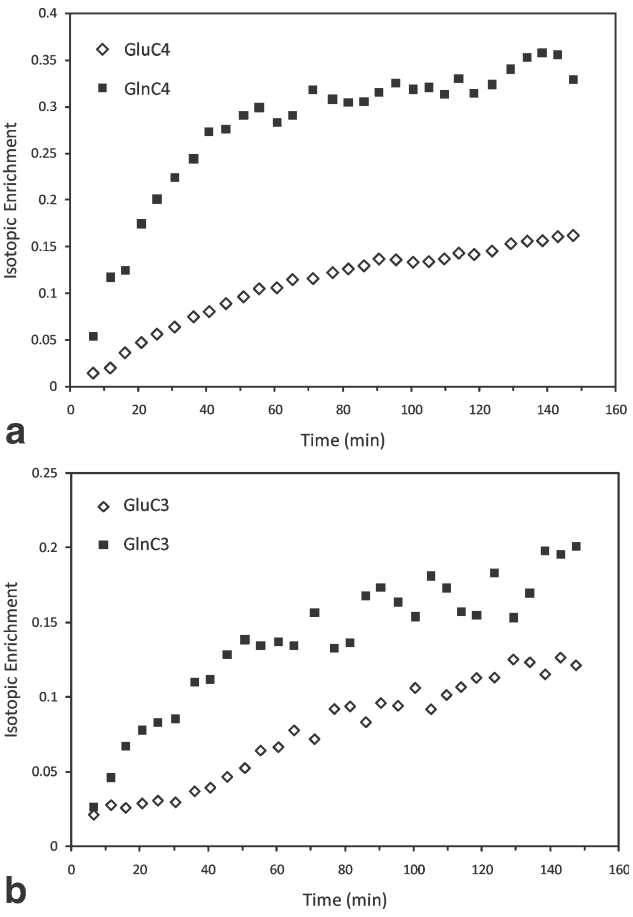

FIG. 5. Average time courses of GlnC4 (**(a)**, closed square), GluC4 (**(a)**, open diamond), GlnC3 (**(b)**, closed square), and GluC3 (**(b)**, open diamond), with 4.5-min time resolution during 150-min [2-^{13}C] Ace infusion (n = 6).

amplitude of radiofrequency field typically present at high magnetic field strength. In contrast to a proton-observed carbon-edited sequence (7), the BISEP ^{13}C editing block generates inverted and noninverted magnetization along the z axis prior to the localization. Therefore, ^{13}C editing is independent of the subsequent localization part, which allows one to combine the BISEP with any localization sequence or spectral editing sequence used for the detection of specific metabolites.

Four scans in total were necessary for accomplishing ^{13}C-localized editing in the proposed scheme. Compared to the proton-observed carbon-edited type of ^{1}H-[^{13}C] NMR sequence combined with three-dimensional image-selected in vivo spectroscopy localization (25), which requires the addition and subtraction of 16 scans, the proposed approach is based on four times fewer add-subtract steps. In addition, outer volume suppression in all three localization dimensions further minimizes the potential contamination from the tissue outside the VOI (volume of interest) caused by add-subtract scheme. This is expected to lead to a more robust detection of ^{13}C label.

In the unedited ^{1}H-[^{13}C] NMR spectra, LCModel was used to analyze the spectrum (33). Moreover, instead of using a TE of 7.9 ms ($1/J_{CH}$) as in the proton-observed carbon-edited type of editing sequence, an ultrashort TE of 2.8 ms was used, which minimized the spectral modulation and signal reduction due to ^{1}H-^{1}H J coupling. This had the advantage that a standard, preexisting basis set including a measured macromolecule baseline was directly used for quantifying the unedited ^{1}H spectra in LCModel analysis.

When using [2-^{13}C] Ace as a substrate, the smaller glial Gln pool is labeled prior to the larger neuronal Glu pool. Substantial dilution of Glu by unlabeled carbon from the more active neuronal TCA cycle leads to a lower isotopic enrichment of metabolites compared to using [1-^{13}C] or [1,6-$^{13}C_2$] glucose as a substrate. Therefore, it was important to optimize the sensitivity of the measurement, which was accomplished in this study by using full-sensitivity ^{1}H-[^{13}C] NMR spectroscopy and by taking advantage of ~50% increase in sensitivity at 14.1 T compared to 9.4 T (34).

Since the field inhomogeneity increases with magnetic field strength, implementation of an efficient automatic shimming scheme such as FASTMAP was crucial to establish high spectral quality. In this study, the typical line width of singlets (total creatine at 3.03 ppm) after the first- and second-order shimming adjustment was 17-18 Hz for a VOI of 144 μL. Although the line width of singlets was increased at 14.1 T compared to 9.4 T, the line width of J-coupled metabolites such as Glu and Gln is determined by the J-coupling constant and thus hardly affected by the increased amplitude of static field (Fig. 2). Hence, the improvement in the chemical shift dispersion was prominent for J-coupled resonances at 14.1 T, e.g., GluC3, which clearly showed a better-resolved doublet structure in the simulated ^{1}H spectrum and in vivo ^{13}C-edited ^{1}H NMR spectra (Fig. 2 and Fig. 3) compared to the lower magnetic field strength (23), as well as a clear separation of GlnC4 and GluC4. Therefore, this study allowed for the first time a separate measurement of time courses of GluC3 and GlnC3 by ^{1}H-[^{13}C] NMR spectroscopy (Fig. 5). These two extra time courses are likely to improve the reliability of metabolic modeling for assessing metabolic fluxes (20).

The accuracy of quantification of the spectra was mainly determined by the quality of the spectra in terms of signal-to-noise ratio and spectral dispersion, which are reflected in Cramer-Rao lower bounds of the metabolite concentrations calculated by LCModel. At 14.1 T, the improved signal-to-noise ratio and separation in Glu and Gln resonances led to ~50% lower Cramer-Rao lower bounds for GluC4, C3 and GlnC4, C3 compared to those at 9.4 T (38).

Although LCModel analysis was used in this study, the improved spectral resolution at 14.1 T, such as resolved GluC4 and GlnC4 resonances, as well as the distinct spectral pattern of GluC3 and GlnC3, should also permit the use of other quantification methods, e.g., jMRUI (magnetic resonance user interface) (39) or constrained peak fitting.

The ^{13}C-labeled metabolites (Fig. 3) detected during [2-^{13}C] Ace infusion observed in this study were similar to those observed under glucose infusion (23). Nevertheless, the turnover pattern of Glu and Gln obtained with [2-^{13}C] Ace infusion was significantly different with that acquired with infusing ^{13}C-enriched glucose. Glutamine labeling showed a faster increase in both C3 and C4 position relative to Glu-labeling time courses. Isotopic enrichment of GlnC4 at steady state was ~2.2 times higher than that of GluC4 (Fig. 4). The isotopic enrichments obtained in the present study were similar to those reported by Deelchand et al. (22), i.e., GluC4 (14%) and GlnC4 (44%).

The high sensitivity achieved from a VOI of 144 μL with a temporal resolution of ~4.5 min under Ace infusion at 14.1 T indicates that at such a magnetic field strength, the proposed sequence could be used to study the ^{13}C turnover in a smaller, more specific brain region. Moreover, with [1-^{13}C]-, [U-$^{13}C_6$]-, or [1,6-$^{13}C_2$]-labeled glucose as a substrate, studies of separate GluC3 and GlnC3 time courses and even time courses of other low-concentration metabolites should be feasible using the described ^{1}H-[^{13}C] NMR technique at 14.1 T.

Ace has been infused in humans but with a lower infusion rate (e.g., 3 mg/kg/min) (11,14); hence, the proposed approach should be of advantage for human studies. The SPECIAL localization sequence and BIR-4 pulses as a part of the FAST(EST)MAP are currently used on our clinical 3- and 7-T scanners (40). It should be straightforward to include a ^{13}C π pulse into BISEP. Provided that sufficient radiofrequency power can be delivered for ^{13}C decoupling within SAR guidelines, the proposed approach can be extended to human studies.

CONCLUSION

We conclude that the ^{1}H-[^{13}C] NMR sequence SPECIAL-BISEP provides a versatile scheme of measuring ^{13}C labeling through protons, with full signal sensitivity. Separate measurements of time-resolved GluC4, GlnC4, GlnC3, and GluC3 are possible at 14.1 T, which likely improves the ability to study neuron-glial metabolism.

ACKNOWLEDGMENTS

The authors thank Dr. Giulio Gambarota for helping with the preparation of the manuscript and Dr. Paul Vasos for helping with the measurement at the high-resolution spectrometer. The work was supported by Centre d'Imagerie BioMédicale of the University of Lausanne (UNIL), University of Geneva (UNIGE), Hôpitaux Universitaires de Genève (HUG), Centre Hospitalier Universitaire Vaudois (CHUV) and Ecole Polytechnique Federale de Lausanne (EPFL), the Leenaards, Jeantet Foundations and Swiss National Science Foundation (SNSF 3100A0-116220).

REFERENCES

1. de Graaf RA, Mason GF, Patel AB, Behar KL, Rothman DL. In vivo ^{1}H-[^{13}C]-NMR spectroscopy of cerebral metabolism. NMR Biomed 2003;16:339–357.
2. Gruetter R, Adriany G, Choi IY, Henry PG, Lei H, Oz G. Localized in vivo ^{13}C NMR spectroscopy of the brain. NMR Biomed 2003;16: 313–338.
3. Sibson NR, Dhankhar A, Mason GF, Behar KL, Rothman DL, Shulman RG. In vivo ^{13}C NMR measurements of cerebral glutamine synthesis as evidence for glutamate-glutamine cycling. Proc Natl Acad Sci U|S|A 1997;94:2699–2704.
4. Henry PG, Adriany G, Deelchand D, Gruetter R, Marjanska M, Oz G, Seaquist ER, Shestov A, Ugurbil K. In vivo ^{13}C NMR spectroscopy and metabolic modeling in the brain: a practical perspective. Magn Reson Imaging 2006;24:527–539.
5. Gruetter R, Seaquist ER, Ugurbil K. A mathematical model of compartmentalized neurotransmitter metabolism in the human brain. Am J Physiol Endocrinol Metab 2001;281:E100–112.
6. Gruetter R, Novotny EJ, Boulware SD, Mason GF, Rothman DL, Shulman GI, Prichard JW, Shulman RG. Localized ^{13}C NMR spectroscopy in the human brain of amino acid labeling from D-[1-^{13}C]glucose. J Neurochem 1994;63:1377–1385.
7. Rothman DL, Behar KL, Hetherington HP, den Hollander JA, Bendall MR, Petroff OA, Shulman RG. ^{1}H-observe/^{13}C-decouple spectroscopic measurements of lactate and glutamate in the rat brain in vivo. Proc Natl Acad Sci U|S|A 1985;82:1633–1637.
8. Badar-Goffer RS, Bachelard HS, Morris PG. Cerebral metabolism of acetate and glucose studied by ^{13}C-N.M.R. spectroscopy: a technique for investigating metabolic compartmentation in the brain. Biochem J 1990;266:133–139.
9. Cerdan S, Kunnecke B, Seelig J. Cerebral metabolism of [1,2-^{13}C2]acetate as detected by in vivo and in vitro ^{13}C NMR. J Biol Chem 1990; 265:12916–12926.
10. Taylor A, McLean M, Morris P, Bachelard H. Approaches to studies on neuronal/glial relationships by ^{13}C-MRS analysis. Dev Neurosci 1996;18:434–442.
11. Lebon V, Petersen KF, Cline GW, Shen J, Mason GF, Dufour S, Behar KL, Shulman GI, Rothman DL. Astroglial contribution to brain energy metabolism in humans revealed by ^{13}C nuclear magnetic resonance spectroscopy: elucidation of the dominant pathway for neurotransmitter glutamate repletion and measurement of astrocytic oxidative metabolism. J Neurosci 2002;22:1523–1531.
12. Bluml S, Moreno-Torres A, Shic F, Nguy CH, Ross BD. Tricarboxylic acid cycle of glia in the in vivo human brain. NMR Biomed 2002;15: 1–5.
13. Chassain C, Bielicki G, Donnat JP, Renou JP, Eschalier A, Durif F. Cerebral glutamate metabolism in Parkinson's disease: an in vivo dynamic (13)C NMS study in the rat. Exp Neurol 2005;191:276–284.
14. Mason GF, Petersen KF, Lebon V, Rothman DL, Shulman GI. Increased brain monocarboxylic acid transport and utilization in type 1 diabetes. Diabetes 2006;55:929–934.
15. Patel AB, de Graaf RA, Mason GF, Rothman DL, Shulman RG, Behar KL. The contribution of GABA to glutamate/glutamine cycling and energy metabolism in the rat cortex in vivo. Proc Natl Acad Sci U|S|A 2005;102:5588–5593.
16. Yang J, Li SS, Bacher J, Shen J. Quantification of cortical GABA-glutamine cycling rate using in vivo magnetic resonance signal of [2-^{13}C]GABA derived from glia-specific substrate [2-^{13}C]acetate. Neurochem Int 2007;50:371–378.
17. Deelchand DK, Nelson C, Shestov AA, Ugurbil K, Henry PG. Simultaneous measurement of neuronal and glial metabolism in rat brain in vivo using co-infusion of [1,6-^{13}C2]glucose and [1,2-^{13}C2]acetate. J Magn Reson 2009;196:157–163.
18. Waniewski RA, Martin DL. Preferential utilization of acetate by astrocytes is attributable to transport. J Neurosci 1998;18:5225–5233.
19. Ottersen OP, Zhang N, Walberg F. Metabolic compartmentation of glutamate and glutamine: morphological evidence obtained by quantitative immunocytochemistry in rat cerebellum. Neuroscience 1992; 46:519–534.
20. Shestov AA, Valette J, Ugurbil K, Henry PG. On the reliability of (13)C metabolic modeling with two-compartment neuronal-glial models. J Neurosci Res 2007;85:3294–3303.
21. Pfeuffer J, Tkac I, Provencher SW, Gruetter R. Toward an in vivo neurochemical profile: quantification of 18 metabolites in short-echo-time (1)H NMR spectra of the rat brain. J Magn Reson 1999;141:104–120.
22. Deelchand DK, Shestov AA, Koski DM, Ugurbil K, Henry PG. Acetate transport and utilization in the rat brain. J Neurochem 2009; 109(suppl 1):46–54.
23. Pfeuffer J, Tkac I, Choi IY, Merkle H, Ugurbil K, Garwood M, Gruetter R. Localized in vivo ^{1}H NMR detection of neurotransmitter labeling in rat brain during infusion of [1-^{13}C] D-glucose. Magn Reson Med 1999;41:1077–1083.
24. Mason GF, Pan JW, Chu WJ, Newcomer BR, Zhang Y, Orr R, Hetherington HP. Measurement of the tricarboxylic acid cycle rate in human grey and white matter in vivo by ^{1}H-[^{13}C] magnetic resonance spectroscopy at 4.1T. J Cereb Blood Flow Metab 1999;19:1179–1188.
25. de Graaf RA, Brown PB, Mason GF, Rothman DL, Behar KL. Detection of [1,6-^{13}C2]-glucose metabolism in rat brain by in vivo ^{1}H-[^{13}C]-NMR spectroscopy. Magn Reson Med 2003;49:37–46.
26. Henry PG, Tkac I, Gruetter R. ^{1}H-localized broadband ^{13}C NMR spectroscopy of the rat brain in vivo at 9.4 T. Magn Reson Med 2003;50: 684–692.
27. de Graaf RA, Mason GF, Patel AB, Rothman DL, Behar KL. Regional glucose metabolism and glutamatergic neurotransmission in rat brain in vivo. Proc Natl Acad Sci U|S|A 2004;101:12700–12705.
28. Tkac I, Andersen P, Adriany G, Merkle H, Ugurbil K, Gruetter R. In vivo ^{1}H NMR spectroscopy of the human brain at 7 T. Magn Reson Med 2001;46:451–456.
29. Mlynarik V, Gambarota G, Frenkel H, Gruetter R. Localized short-echo-time proton MR spectroscopy with full signal-intensity acquisition. Magn Reson Med 2006;56:965–970.
30. Garwood M, Merkle H. Heteronuclear spectral editing with adiabatic pulses. J Magn Reson 1991;94:180–185.
31. Tkac I, Starcuk Z, Choi IY, Gruetter R. In vivo ^{1}H NMR spectroscopy of rat brain at 1 ms echo time. Magn Reson Med 1999;41:649–656.
32. Gruetter R, Tkac I. Field mapping without reference scan using asymmetric echo-planar techniques. Magn Reson Med 2000;43: 319–323.
33. Provencher SW. Estimation of metabolite concentrations from localized in vivo proton NMR spectra. Magn Reson Med 1993;30:672–679.
34. Mlynarik V, Cudalbu C, Xin L, Gruetter R. ^{1}H NMR spectroscopy of rat brain in vivo at 14.1 tesla: improvements in quantification of the neurochemical profile. J Magn Reson 2008;194:163–168.
35. Gambarota G, van der Graaf M, Klomp D, Mulkern RV, Heerschap A. Echo-time independent signal modulations using PRESS sequences: a new approach to spectral editing of strongly coupled AB spin systems. J Magn Reson 2005;177:299–306.
36. Govindaraju V, Young K, Maudsley AA. Proton NMR chemical shifts and coupling constants for brain metabolites. NMR Biomed 2000;13:129–153.
37. Xin L, Frenkel H, Mlynarik V, Morgenthaler FD, Gruetter R. Selective resonance suppression ^{1}H-[^{13}C] NMR spectroscopy with asymmetric adiabatic RF pulses. Magn Reson Med 2009;61:260–266.
38. Xin L, Mlynárik V, Frenkel H, Gruetter R. Comparison of glutamate and glutamine quantitation in rat brain by ^{1}H–[^{13}C] NMR spectroscopy at 9.4 T and 14.1 T. In: Proceedings of the 26th Annual Meeting of ESMRMB, Antalya, Turkey, 2009. p 324.
39. Naressi A, Couturier C, Castang I, de Beer R, Graveron-Demilly D. Java-based graphical user interface for MRUI, a software package for quantitation of in vivo/medical magnetic resonance spectroscopy signals. Comput Biol Med 2001;31:269–286.
40. Mekle R, Mlynarik V, Gambarota G, Hergt M, Krueger G, Gruetter R. MR spectroscopy of the human brain with enhanced signal intensity at ultrashort echo times on a clinical platform at 3T and 7T. Magn Reson Med 2009;61:1279–1285.